Phylosymbiosis shapes skin bacterial communities and pathogen-protective function in Appalachian salamanders

Osborne, Owen; Jiménez, Randall; Byrne, Allison; Gratwicke, Brian; Ellison, Amy; Muletz-Wolz, Carly

The ISME Journal

DOI:
10.1093/ismejo/wrae104

Published: 11/06/2024

Peer reviewed version

Phylosymbiosis shapes skin bacterial communities and pathogen-protective function in Appalachian salamanders

Running head: Phylosymbiosis in salamanders

Authors: Owen G. Osborne[1*], Randall R. Jiménez[2,3], Allison Q. Byrne[2,4], Brian Gratwicke[5], Amy Ellison[1], Carly R. Muletz-Wolz[2*]

Affiliations:

[1]School of Environmental and Natural Sciences, Bangor University, Bangor, Gwynedd, LL57 2DG, UK

[2]Center for Conservation Genomics, Smithsonian's National Zoological Park and Conservation Biology Institute, Washington, DC, USA

[3]International Union for Conservation of Nature, San Jose, Costa Rica

[4]Department of Environmental Science, Policy & Management, University of California, Berkeley, CA, USA

[5]Center for Species Survival, Smithsonian's National Zoological Park and Conservation Biology Institute, Front Royal, VA, USA

[*]Authors for correspondence: owengosborne@gmail.com and muletzc@si.edu.

Funding information: The work was funded by a Smithsonian Scholarly Studies grant to CRMW and BG and an NSF (USA) – BBSRC (UK) grant to CRMW, AE and BG (NSF IOS-2131060 and BBSRC BB/W013517/1).

Abstract

Phylosymbiosis is an association between host-associated microbiome composition and host phylogeny. This pattern can arise via evolution of host traits, habitat preferences, diets, and co-diversification of hosts and microbes. Understanding the drivers of phylosymbiosis is vital for modelling disease-microbiome interactions and manipulating microbiomes in multi-host systems. This study quantifies phylosymbiosis in Appalachian salamander skin in the context of infection by the fungal pathogen *Batrachochytrium dendrobatidis* (Bd), while accounting for environmental microbiome exposure. We sampled ten salamander species representing >150M years divergence, assessed their Bd infection status, and analysed their skin and environmental microbiomes. Our results reveal a significant signal of phylosymbiosis, whereas the local environmental pool of microbes, climate, geography, and Bd infection load had a smaller impact. Host-microbe co-speciation was not evident, indicating that the effect stems from the evolution of host traits influencing microbiome assembly. Bd infection correlated with host phylogeny and the abundance of Bd-inhibitory bacterial strains, suggesting that the long-term evolutionary dynamics between salamander hosts and their skin microbiomes affects the present-day distribution of the pathogen, alongside habitat-linked exposure risk. Five Bd-inhibitory bacterial strains showed unusual generalism: occurring on most host species and habitats. These generalist strains may enhance the likelihood of probiotic manipulations colonising and persisting on hosts. Our results underscore the substantial influence of host-microbiome eco-evolutionary dynamics on environmental health and disease outcomes.

Keywords

Phylosymbiosis; *Batrachochytrium dendrobatidis*; *Batrachochytrium salamandrivorans*; Host-microbiome interactions; Community assembly; Probiotics

Introduction

Host-associated microbiomes are ecosystems structured by a combination of deterministic and stochastic processes [1–5]. Compared to other complex multispecies assemblages, host-associated microbiomes are unique in that assembly processes act at both host environment and host biology levels [6]. The environment of the host often affects the regional pool of microbial species that exist as potential colonisers [7]. In host-associated microbiomes, microbes are colonising a living organism, and a secondary ecological filter operates at the host biology level (Fig. 1). This could relate to host species or host site such as a plant root or an animal skin [8]. Host filtering may involve traits that are evolutionarily conserved or subject to divergent selection between host species. Using an integrated approach to examine environmental and host microbiomes in evolutionary diverse host species communities will allow us to more accurately quantify the processes that underpin host-associated microbiome assembly.

In host-associated microbiome research, individuals within the same species have most often been sampled in multiple localities as a proxy for different environmental exposures. Generally, environment has been found to influence microbiomes in a variety of plant [9, 10] and animal systems, including skin microbiomes [11, 12]. Although these studies have been powerful in demonstrating the role of the environment, few studies have characterized the microbiome of the host's environment in parallel with that of the host microbiome. Integration of environmental microbiomes with host microbiomes provides critical insight into the role of environmental transmission of microbiota from environment to host [7], which can impact host ecology [13] and health [14].

Host biology is often important in predicting microbial composition and microbiomes typically differ between species [4, 5, 11]. These differences sometimes mirror host evolutionary history – a pattern termed phylosymbiosis – whereby microbiome dissimilarity is correlated with host phylogenetic distance [15, 16]. Phylosymbiosis has been observed in vertebrate gut [17, 18] and skin microbiomes [19–21], internal plant microbiomes [22], and many other systems [16]. Host-microbe co-speciation accounts for phylosymbiosis in some cases [23]. However, mechanisms of ecological filtering by host traits can mirror evolutionary history and explain phylosymbiosis [24], such as co-variation between host diet or life history and phylogeny [25, 26]. Although phylosymbiosis has been demonstrated in multiple systems, the mechanisms underlying it, and particularly the influence of host life history, are poorly understood.

The eco-evolutionary processes shaping host-associated microbiomes may have significant practical implications for biodiversity conservation. The emerging field of wildlife probiotics [27] has the potential to effectively mitigate wildlife outbreaks, and probiotics have been applied to multiple animal diseases including white-nose syndrome in bats [28], chytridiomycosis in amphibians [29], and American foulbrood in honeybees [30]. For these interventions to be effective however, some degree of persistence of the introduced probiotics is required, and this is likely to be largely dependent on the host-microbiome interactions which play out in wild settings. Therefore, understanding the dynamics of host-associated microbiome specificity and host-microbe co-evolution is crucial for designing effective microbiome-manipulation strategies to combat pathogen-mediated biodiversity loss.

Among vertebrates, amphibian skin is an important system to examine environmental and host evolutionary effects on microbiome assembly [31]. Amphibian skin lacks protective fur or feathers and is covered with a moist mucus layer which can act as a bacterial substrate [31]. Furthermore, in contrast to other vertebrate classes, amphibian skin is a critical respiratory and osmoregulatory organ [31]. It also plays an important role in innate immunity, hosting an extremely diverse array of antimicrobial peptides [32]. Thus, amphibians are particularly sensitive to skin microbiome perturbations but are equipped with unique adaptations to influence their skin microbiome composition.

The Appalachian Mountains are rich in salamander species diversity, with more than 75 species in 14 genera. These are dominated by members of the family Plethodontidae, but represent more than 150M years of evolution in total [33, 34]. These species also differ widely in life histories, ranging from fully aquatic to fully terrestrial species, with many species co-occurring. Further, amphibians are impacted by the chytrid fungal pathogens (*Batrachochytrium dendrobatidis* [Bd] and *Batrachochytrium salamandrivorans* [Bsal]), which can infect their skin and cause the disease chytridiomycosis [35]. Not all amphibian species are equally susceptible and skin microbiomes play an important role in Bd infection probability and disease outcomes [4, 36]. Together, the high species diversity, range in environmental exposures, and the pathogen-protective traits of the skin microbiome make Appalachian salamanders a useful study system to examine the effects of environment, life history, pathogen susceptibility, and evolutionary history on host microbiome assembly.

Here, we studied the environmental and host skin-associated bacteria from 10 wild salamander species in the Central Appalachians, USA. Specifically, we aimed to (i) investigate the roles of geographic locality, habitat and host-species in salamander-associated microbial community structure; (ii) determine whether, and by what mechanism, skin microbiomes follow a pattern of phylosymbiosis in salamanders; (iii) determine whether these host-microbiome eco-evolutionary processes affect disease dynamics via Bd-protective bacteria in wild salamanders; and (iv) explore whether this information can be used to develop more effective pathogen mitigation strategies. Integrating evolutionary history and environmental microbiomes into a unified framework allows us to identify how these combined factors impact host-associated microbiomes and organismal and environmental health.

Methods

Sample collection

We sampled 10 species of salamander at 12 sites within three localities in Maryland and Virginia, USA in October 2020 (permit details: Supplementary Methods 1). This included species: *Ambystoma jeffersonianum* (5 samples; 1 site), *Desmognathus fuscus* (11 samples; 3 sites), *D. monticola* (2 samples; 1 site), *D. ochrophaeus* (13 samples; 2 sites), *Eurycea bislineata* (53 samples; 5 sites), *Gyrinophilus porphyriticus* (5 samples; 2 sites), *Notophthalmus viridescens* (77 samples; 6 sites), *Plethodon cinereus* (57 samples; 5 sites), *P. glutinosus* (6 samples; 2 sites), and *P. hoffmani* (2 samples; 2 sites; Fig. 2; Tables S1-S2). Salamanders and their environment were sampled from one or more of three broad habitats at each site: pond, stream, or forest (Table S1). Salamanders were captured by dip-netting (ponds) and visual encounter surveys by flipping logs and rocks (streams and forest) at each of the sites. Each

captured salamander was swabbed for disease quantification and microbiome profiling, before being released. Environmental samples from aquatic and terrestrial environments were collected from substrate (water for aquatic or soil for terrestrial samples) near where salamanders were captured (Supplementary Methods 2).

Pathogen and microbiome molecular methods

Genomic DNA was extracted from skin swabs using the DNeasy PowerSoil HTP 96 kit (Qiagen). We used qPCR for the quantification of Bd, Bsal and ranavirus infection using synthesized gene fragments (gBlocks; Integrated DNA) as in [37] and report Bd loads as Bd copies per swab. Based on previous studies, loads above 10,000 copies were considered high and suggestive of a diseased state [38, 39]. All swabs were tested in duplicate. We used a two-step PCR library preparation and dual-index paired-end sequencing to sequence the skin microbiome of each salamander skin swab sample, positive and negative controls. Briefly, we amplified the V3-V5 region of the 16S rRNA gene (~380 bp) using the universal primers 515F-Y and 939R [4, 5], and sequenced the libraries on two MiSeq (Illumina) runs at the Center for Conservation Genomics, NZCBI (Supplementary Methods 3).

Sequence processing

Raw data processing followed a previous study [4], using the *dada2* [40], *MAFFT* [41], *FastTree* [42], *QIIME 2* [43], *phyloseq* [44], and *decontam* [45] software packages and taxonomic identification using the Ribosomal Database Project [46] database (Supplementary Methods 4). Our sequencing produced a total of 12,217,181 sequences with an average of 34,031 read pairs per sample (Table S2). A rarefied dataset was created by rarefying at an even depth of 2,945 reads, which was chosen

to capture the diversity present while retaining as many samples as possible (Fig. S1). This was used to account for uneven sampling depths in some downstream analyses (noted below). All ASV sequences were BLASTn searched against the Anti-fungal Isolates Database [47] (updated database received from M. Bletz July 2022). ASVs with 100% identity to known Bd-inhibitory isolates from the database were considered to have putative Bd-inhibitory activity.

Microbial diversity analyses

We estimated alpha diversity (ASV richness) using the rarefied dataset. To determine whether alpha-diversity significantly differed according to locality, habitat, and host species, we used Scheirer-Ray-Hare tests [48] (SRH tests; used due to inequality of variance between groups) implemented in the R package *rcompanion* [49]. To circumvent the confounding effect of species and habitat in salamander samples, we only compared species within the same habitat category in habitat subsets (Supplementary Methods 5). One species was found in both pond and forest habitats as adults, *N. viridescens*, and was analysed as a species subset to examine locality and habitat effects within a species (Supplementary Methods 5). For all significant factors with more than two levels in the SRH tests, we conducted post-hoc Dunn's tests implemented in the R package *FSA* [50] to determine which groups significantly differed (Supplementary Methods 5). We also estimated alpha diversity of Bd-inhibitory ASV and correlated Bd-inhibitory ASV richness with total ASV richness using a linear model (LM).

We estimated beta diversity (from the rarefied dataset) between all sample pairs using the Jaccard, Bray-Curtis, unweighted UniFrac, and weighted UniFrac metrics. We then

used PermanovaG tests implemented in the *GUniFrac* R package [51], which allowed all four beta-diversity metrics to be combined in a single omnibus test, to test differences in bacterial community composition associated with locality, habitat, and host species (with species examined within habitat-specific subsets as in alpha diversity; Supplementary Methods 5). For significant *PermanovaG* tests, we conducted post-hoc testing using pairwise *PermanovaG* to determine which groups significantly differed (with *P* values corrected using FDR). Community composition differences were visualised using Nonmetric Multidimensional Scaling (NMDS).

Phylosymbiosis analyses

To determine whether microbial community distance showed a signal of phylosymbiosis, we used both Mantel test and tree-based methods. We also tested for an association between mean univariate microbial traits (ASV richness, Bd-inhibitory bacterial richness and relative abundance, Bd prevalence and Bd load) using the function *multiPhylosignal* in the R package *picante* [52, 53]. To determine whether phylogenetic signal in these traits were robust to intraspecific variability, we used a bootstrapping approach. For each bootstrap replicate, we resampled each species with replacement maintaining the original number of samples per species, recalculated each mean trait, and re-ran the *multiPhylosignal* test. This was repeated 1,000 times and *P* values for all replicates were combined using the Cauchy combination method [54]. For phylosymbiosis analyses, we implemented all tests using each of the four beta-diversity measures of salamander skin calculated above, separately. We first extracted a dated phylogeny for all host species from TimeTree [55] (downloaded: 31 July 2023; TimeTree synthesises multiple published phylogenies, in this case 16) and extracted host phylogenetic distance using the *cophenetic* function in the R package

ape [56]. Mantel tests were conducted at both the sample and species level and a tree-based permutation test was implemented with the *cospeciation* function in the R package *phytools* [57] (Supplementary Methods 6).

To quantify the effect of host phylogeny and environmental variables on the salamander skin microbiome, we used multiple regression on distance matrices [58, 59] (MRM) implemented in the *MRM* function in the R package *ecodist* [60]. Our MRM model included five predictor variables: host phylogenetic distance, geographic distance, climatic distance, environmental microbiome distance, and Bd infection load distance which were standardised, so the analysis resulted in comparable standardised regression coefficients (β; Supplementary Methods 7). To determine whether Bd-inhibitory strains showed a similar pattern of phylosymbiosis to the general microbiome, phylosymbiosis and MRM analyses were repeated using only the Bd-inhibitory subset of taxa.

The species are geographically and habitat restricted, and some bacterial taxa may only be present in certain habitats or geographic regions. Phylosymbiosis could therefore plausibly result from habitat and range differences coinciding between host and bacterial species. We addressed this possibility through two approaches. Firstly, to test whether differential presence-absence of bacteria between localities and habitats drives phylosymbiosis, we produced a “global-ASVs” dataset by filtering the salamander microbiome dataset to include only ASVs which were present in all locality-habitat combinations (in either environmental or skin salamander skin samples in the pre-rarefied data; 66 ASVs). All phylosymbiosis tests and MRM analyses were then repeated with this dataset. Secondly, to determine whether phylosymbiosis was

evident when the influence of habitat was removed, we repeated the individual-level Mantel tests and MRM analysis on subsets containing only species from stream and forest habitats separately (pond species were not used in this analysis because only two were sampled).

One mechanism which may lead to phylosymbiosis is co-speciation of hosts and vertically acquired microbes during diversification [61]. To determine whether this process contributes to phylosymbiosis in the salamander skin microbiome, we used the ParaFit [62] method (Supplementary Methods 8).

Specificity analysis

To quantify the specificity of ASVs in the salamander skin microbiome to host phylogeny, environment, and Bd load, we used the method implemented in the *specificity* R package [63]. This approach indicates whether ASVs occupy a narrower (or broader) range of an environmental variable than expected by chance using the convenient Rao's Quadradic Entropy [64, 65], which allows calculation of specificity for both linear and higher-dimensional variables. We calculated specificity to five explanatory variables used in the MRM analysis. Using the rarefied dataset, ASVs occurring in fewer than 10 samples were removed (as recommended by the authors). We calculated specificity indices and *P* values for all remaining ASVs, and calculated mean specificity indices for all branches of the bacterial phylogeny, which were visualised with heat trees implemented in the R package *metacoder* [66]. Specificity indices were examined for putative Bd-inhibitory ASVs to identify strains which may have good potential to become established when introduced to novel host

environments, and thus be promising candidates for probiotic approaches to control Bd.

Relationship between Bd infection and microbiome structure

To identify ASVs which significantly differed between Bd infected and non-infected individuals we conducted differential abundance analysis implemented in the *DESeq2* R package [67, 68]. This was conducted at the ASV level, using the model formula "~Species_Habitat + Locality + $Bd_{infection}$" where Species_Habitat is a combined factor of Species and Habitat, Locality is geographic locality, and $Bd_{infection}$ indicates whether salamanders were infected or not. Corrected *P* values were then extracted for the Bd infected versus non-infected contrast. To account for the high sparsity of the ASV level data, we used the "poscounts" method for estimating size factors (used to correct for different library sizes between samples). We cross-referenced all ASVs to the putatively anti-Bd ASV set. We determined whether these were significantly over-represented among significant ASVs using a Fisher's Exact Test.

Results

Microbial diversity is associated with geography, habitat, and host species.

After filtering ASVs and removing low read-count and control samples, 118 environmental and 222 salamander samples remained with between 23 and 973 ASVs (Table S2). We first assessed the effects of locality, habitat, and species on environmental and skin microbiome structure. Generally, environmental microbiome structure (Figs. 3, 4A-C) differed among localities (alpha and beta diversity) and habitats (beta diversity), and salamander skin microbiome structure (Figs 3, 4A-C) differed among localities (beta diversity), habitats (alpha and beta diversity), and

297 salamander species (alpha and beta diversity; Tables S3-S6). Salamanders living in
298 ponds had markedly lower bacterial diversity on their skin, but this was not observed
299 in environmental samples (Fig. 3; Table S3). One species, *N. viridescens*, was present
300 in two habitats, and showed lower alpha diversity and distinct bacterial composition
301 (beta diversity) in ponds as aquatic adults compared to terrestrial adults in the forest
302 (Table S3). For environmental samples, Mountain Maryland environments had
303 significantly higher alpha diversity than the other two localities (Table S4), whereas
304 bacterial community composition significantly differed among all localities and habitats
305 (Fig. 4A-C; Fig. S2; Table S5; Table S6). Bd-inhibitory bacterial richness was
306 correlated with total ASV richness on salamander skin and in the environment (LM: P
307 < 0.001), but the relationship was stronger on salamander skin (R^2 skin = 0.50,
308 environment = 0.11). For salamander samples, bacterial community composition
309 significantly differed among all three localities (Table S5, S6) and species in all three
310 habitat subsets (Table S5). Eight species pairs from a total of 17 tested were
311 significantly different in the post-hoc tests (Table S6). Except for *D. fuscus* and *D.*
312 *ochrophaeus*, all significant pairs were from different genera, implying that greater host
313 phylogenetic distance may be associated with higher microbiome divergence, a
314 hypothesis that we then tested explicitly.
315
316 *Skin microbiome distance recapitulates host phylogeny*
317 We found a strong pattern of phylosymbiosis in the skin microbiome of Appalachian
318 salamanders (Fig. 4D-E). We likewise found phylogenetic signal in bacterial ASV
319 richness, Bd-inhibitory bacterial richness, and Bd load, and a near significant effect in
320 Bd prevalence, all of which remained significant when we accounted for intraspecific
321 variation (Table S7). In our phylosymbiosis analyses, individual-level Mantel tests

were significant ($P < 0.0001$) for all four beta-diversity metrics. Species-level Mantel tests were all significant apart from with weighted UniFrac ($P = 0.0511$; Table S8). Tree-based permutation tests were consistently significant (Table S8). We obtained similar results when using only the subset of Bd-inhibitory ASVs (Table S8). When we calculated beta-diversity statistics using only the set of ASVs present in all habitat-locality combinations (66 global-ASVs), the pattern of phylosymbiosis remained (Table S8). Similarly, a significant signal of phylosymbiosis was found (Table S8) and host phylogeny had a significant effect (albeit with a reduced effect size; Table S9) within single-habitat subsets. These results indicated the signal of phylosymbiosis is not derived solely from differences in bacterial presence-absence between the habitats and ranges of the salamander species. The results of the MRM analysis supported this conclusion. Host phylogeny showed a strong (β = [0.48, 0.60]; Fig. 4f; Fig. S3; Table S9) and highly significant ($P < 0.0001$) association with skin microbiome dissimilarity across all beta-diversity metrics. Environmental microbiome distance was also significant for all beta-diversity metrics ($P < 0.0001$) but had a smaller effect size (β = [0.10, 0.21]; Fig. 4f; Table S9). The results for climatic, geographic, and Bd load distance were more inconsistent, with significant effects using some beta diversity metrics but with consistently small effect sizes (Fig. 4f; Table S8). For the subset of Bd-inhibitory ASVs, host phylogeny again showed the strongest association with skin microbiome dissimilarity (β = [0.35, 0.52], $P < 0.0001$). Putatively Bd-inhibitory ASVs were consistently associated with Bd load (β = [0.07, 0.19]), in contrast to the complete dataset (Fig. S3; Table S9).

345 We found no evidence of vertical transmission driving phylosymbiosis in Appalachian
346 salamander skin. Across all four clustering methods, no OTU had a significant
347 phylogenetic signal following multiple test correction (Table S10).
348
349 *Host and environmental specificity*
350 Specificity to host phylogeny, climate distance, geographic distance, environmental
351 microbiome distance, and Bd load varied between microbial phyla (Fig. 5A-B; Figs.
352 S5-S7). The highest number of significantly specific ASVs were found for host
353 phylogeny, followed by environmental microbiome distance (Fig. 4G; Table S11).
354 There were substantially fewer geography and climate specific ASVs, in line with the
355 MRM analysis (Fig. 4F). Of the putative anti-Bd bacteria, five had positive (i.e.
356 generalist) specificity indices for both host and environmental microbiome distance
357 (Fig 5C; Table S11). These were taxonomically identified as *Chryseobacterium* sp.
358 (ASV169, 495), *Iodobacter* sp. (ASV105), *Acinetobacter* sp. (ASV323), and an ASV of
359 unknown genus in the family *Enterobacteriaceae* (ASV1179). The final two of these
360 also had positive indices for both climate and geographic distance (correlation
361 between the different specificity indices was high; Fig. S4), and all were present in a
362 wide range of species and habitats (Fig. 5D). These five taxa may be particularly good
363 candidates for probiotic treatments (e.g [14]) due to their ability to colonise a broad
364 range of salamander species and environments in the wild.
365
366 *Known Bd-inhibitory bacteria are significantly associated with Bd infection status in*
367 *wild salamanders*
368 Bd was found to be widespread in the Appalachian region we sampled, with
369 prevalence ranging from 0% to 65% per species (Fig. 2). Six of the ten salamander

370 species were found to be infected, with *N. viridescens* having the highest prevalence
371 and loads (prevalence: 65%; mean Bd load: 17,317 copies), and *G. porphyriticus*, *P.*
372 *glutinosus*, *D. fuscus*, *E. bislineata*, and *P. cinereus* also found to have at least one
373 individual infected (Fig. 2). No individuals were infected with Bsal or ranavirus. We
374 identified 547 taxa that were differentially abundant between Bd-infected and non-
375 infected individuals while controlling for species, habitat, and locality (Table S11;
376 negative log fold change represents lower abundance in Bd-infected salamanders).
377 These were dominated by *Proteobacteria* (247 ASVs), but also included taxa
378 distributed widely across the bacterial phylogeny, including *Bacteroidetes* (125 ASVs)
379 *Actinobacteria* (80 ASVs), *Acidobacteria* (46 ASVs), and *Verrucomicrobia* (17 ASVs;
380 Table S11). Although many bacteria have been shown to have Bd-inhibitory ability *in*
381 *vitro* [47], these are largely untested in the wild. We therefore cross-referenced the
382 differentially abundant taxa and those with significant specificity to Bd load (see above)
383 with the putatively anti-Bd set of ASVs identified *in vitro* from a previously published
384 database [47]. This revealed that whereas only 3% of ASVs absent from the Bd-
385 inhibitory database were differentially abundant according to Bd infection status, 16%
386 of putatively anti-Bd bacteria were, a highly significant association (Table S12). A
387 similar significant association was found between Bd load specificity and putative anti-
388 Bd activity (Table S12). Of the 22 putative anti-Bd bacteria significantly associated
389 with Bd infection status, 13 ASVs were more abundant in Bd-infected individuals,
390 whereas nine ASVs were more abundant in uninfected individuals. When these were
391 considered separately, the relationship with putative anti-Bd activity remained
392 significant ($P < 0.0001$; Table S12).
393
394 **Discussion**

Microbial diversity plays a crucial role in the health of humans and many animals and plants [69–71]. Determining which factors impact host-associated microbiome structure are critical for issues as diverse as health, food production, and biodiversity conservation [72, 73]. Here, we show that in the world's foremost centre of salamander biodiversity, microbiome composition follows a pattern of phylosymbiosis, is influenced by habitat and that the abundance of many bacterial taxa is linked to pathogen (Bd) infection in the wild. Together, this indicates that salamander skin microbiomes are constrained in their functional capacity by the evolutionary history and environment of the host, and that these eco-evolutionary processes may alter disease dynamics by affecting the distribution of pathogen-protective bacteria.

Phylosymbiosis in Appalachian salamanders is not explained by habitat and range divergence

We provide strong evidence for phylosymbiosis in the skin microbiomes of Appalachian salamanders in overall bacterial composition, putatively Bd-inhibitory bacterial composition, and in widely distributed bacterial composition (global-ASVs). Host phylogeny consistently explained bacterial composition more strongly than environment or the local pool of microbes (Fig. 4F; Table S9). Phylosymbiosis refers to a general pattern where relationships between host-associated microbial communities recapitulate the host phylogeny. The term does not imply a mechanism and may arise via either stochastic processes such as ecological drift and isolation-by-distance or deterministic processes [61]. These can include the evolution of host traits and environmental preferences that affect their microbial community compositions or co-diversification between host and microbes. Simulations have shown that weighted measures detect phylosymbiosis more effectively, potentially

because bacteria that are better adapted to the host environment are likely to be more abundant [24]. We observed greater support for phylosymbiosis in weighted beta diversity measures in the MRM analyses and in Mantel tests for the putatively Bd-inhibitory and global-ASVs datasets, supporting this hypothesis (although not in the Mantel tests of the whole microbiome dataset).

Ecological filtering from the environment may explain patterns of phylosymbiosis [74], but here we account for environmental microbiome contribution and find a far stronger effect from host phylogeny, suggesting a greater role of the evolution of intrinsic host traits on microbiome assembly. A recent study showed phylosymbiosis in salamander skin microbiomes [21], but did not quantify the contribution of environmental microbial community differences due to the absence of environmental microbiome samples. Phylosymbiosis in salamanders contrasts with a previous study in Malagasy frog skin microbiomes, where host ecology was found to be a more important driver than host phylogeny [75]. Drivers of rapid diversification may explain this difference. In Malagasy frogs [76], morphological and microhabitat-niche linked diversification predominates. In Appalachian salamanders, climatic-niche diversification predominates, and morphology and microhabitat use is generally not linked to diversification [77]. Appalachian salamanders may have undergone diversification in host skin traits in response to exposure to climatic-specific environmental microbes. However, we found no evidence for co-speciation between salamander species and microbial symbionts, a result that could be confirmed in future work using metagenomic approaches with greater phylogenetic resolution [61]. This suggests instead that Appalachian salamanders are predominately acquiring their skin microbial symbionts from the environment during an individual's lifetime. Nonetheless, we found that the

environmental pool of microbes had a relatively small effect on the skin microbiome. Taken together, we hypothesise that the evolution of host climatic or habitat preference results in a different pool of microbes which could colonise the host skin, but that the evolution of intrinsic host traits, potentially immunological traits such as antimicrobial peptides (AMPs) [4] and major histocompatibility complex (MHC) molecules [78], has a more important effect, by differentially filtering these microbes between species (Fig. 1; Fig. 4F).

Host-microbe skin interactions are particularly important in relation to skin-associated pathogens such as Bd. We found large differences in Bd prevalence and load between species, with Bd load having a significant phylogenetic signal. Species-specific differences in Bd prevalence and load may result from intrinsic host traits such as MHC genes and AMPs [32, 79] and the differences in skin-associated microbiota as documented here and previously [4, 21], but may also relate to the linkage between evolutionary history and habitat preference in the salamander species we examined. We hypothesize that both evolutionary history and habitat-linked exposure risk explains Bd load dynamics, and not habitat alone. This is supported by i) high Bd susceptibility and Bd-linked decline in terrestrial Plethodontid salamanders [80, 81] and (ii) our observations that Bd infected individuals occurred in all habitats and localities.

We show evidence for evolutionary history predicting the distribution of Bd-inhibitory bacterial richness and composition. We also identified 547 ASVs which were significantly differentially abundant between *Bd* infected and non-infected individuals, suggesting that skin microbiome-Bd dynamics are also operating at more recent time

scales. Strains with known Bd-inhibitory activity *in vitro* were significantly more likely to be differentially abundant between Bd infected and uninfected salamanders. These included strains which were both significantly more and less abundant in infected versus uninfected individuals, hinting at a diversity of mechanisms by which Bd-protective bacteria may benefit hosts in the wild. It is possible that some strains may preclude Bd infection entirely, whereas others may reduce the severity of symptoms in infected individuals. Of the 13 genera of differentially abundant anti-Bd bacteria, only three genera had multiple ASVs that were differentially abundant – *Chryseobacterium*, *Pedobacter* and *Pseudomonas* – and these genera had ASVs that showed both increased and decreased abundance with Bd infection, highlighting the importance of strain level distinctions. Another finding was the low bacterial richness in pond-dwelling salamanders, particularly *N. viridescens*, which also have high Bd prevalence and harbour very high Bd loads. Our results highlight the important links among evolutionary history, environmental and host microbial diversity and disease dynamics [4].

Host-specificity and in vivo effectiveness of putative anti-Bd probiotics

The use of probiotics to improve host health have been applied in fields as diverse as aquaculture [82], crop improvement [83], human health [84] and conservation biology [85]. This includes efforts to harness bacteria with antifungal activity to combat chytridiomycosis in amphibians [86, 87]. This approach may have several advantages over other approaches. For example, long-term establishment of protective bacteria would provide lasting protection without the need for repeated treatments as required with antifungal chemical agents, and the use of bacteria already occurring in the ecosystem would reduce the chance of damaging and unpredictable ecosystem

495 impacts [88]. However, although many bacterial strains have been shown to have anti-
496 Bd activity in-vitro [47], application of these to ameliorate Bd infection in live
497 amphibians has had mixed results [85, 87, 89]. Low colonisation and persistence of
498 anti-Bd bacteria on the host may limit effectiveness [14, 87, 90]. We identify bacteria
499 in our specificity analyses that are more generalist and likely have a greater probability
500 of persisting when introduced to novel hosts or environments (16S sequences
501 available in table S11). These may improve the chance of effective anti-Bd activity in
502 wild populations and may be particularly relevant if Bd sister taxon, Bsal, were to reach
503 Appalachia, as we have previously shown that Bd-inhibitory bacteria also can kill Bsal
504 [91]. Taxa which are known to have generalist distributions (Fig. 5C) may be fruitful
505 targets for future probiotic approaches, specifically *Chryseobacterium* and
506 *Acinetobacter*, which have already been isolated from multiple continents and diverse
507 species [47] and shown to be important in pathogen-microbiome-host interactions [92,
508 93]. Probiotic effectiveness using multiple probiotic strains challenged against diverse
509 clades of Bd and Bsal should be considered in picking ideal strains to focus research
510 efforts [91]. Conversely, taxa from more species-specific clades, such as
511 *Acidobacteria* and *Actinobacteria*, may have a lower chance of being effective as
512 general anti-*Bd* probiotics.
513
514 Here, we show that microbial diversity in Appalachian salamander skin show a strong
515 pattern of phylosymbiosis which likely derives largely from the evolution of intrinsic
516 host traits that select for unique microbial symbionts from the environmental pool.
517 Furthermore, the abundance of multiple microbial taxa is significantly associated with
518 fungal *Bd* infection, including strains which are known to have anti-Bd activity *in vitro*.
519 Our results highlight the importance of the long-term evolutionary dynamics of host-

microbiome interactions in disease susceptibility and suggest potential avenues by which to harness it more effectively in conservation interventions. Deepening our understanding of the complex interactions between pathogen, microbiome, environment, and host immune system that determine disease susceptibility increases our chances of improving disease outcomes for conservation purposes, both for Bd and to combat Bsal, should this sister taxon be introduced into this salamander biodiversity hotspot.

Acknowledgements

The work was funded by a Smithsonian Scholarly Studies grant to CRMW and BG and a joint National Science Foundation (NSF; USA) - Biotechnology and Biological Sciences Research Council (BBSRC; UK) grant to CRMW, AE and BG (NSF IOS-2131060 and BBSRC BB/W013517/1). We would like to thank Mia Keady and Morgan Bragg for help with field work. We would like to thank anyone involved in conserving Appalachian salamander biodiversity.

Data and Code Availability

We deposited demultiplexed sequence data in the National Center for Biotechnology Information Sequence (NCBI) under BioProject ID: PRJNA1039858. All code used for data analysis is available at https://github.com/ogosborne/salamander_phylosymbiosis and all software versions are shown in table S13.

Competing Interests

The authors declare no competing interests.

References

1. Zhou J, Ning D. Stochastic community assembly: Does it matter in microbial ecology? *Microbiol Mol Biol Rev* 2017; **81**: e00002-17.
2. Miller ET, Svanbäck R, Bohannan BJM. Microbiomes as metacommunities: Understanding host-associated microbes through metacommunity ecology. *Trends Ecol Evol* 2018; **33**: 926–935.
3. Grisnik M, Grinath JB, Walker DM. The presence of *Pseudogymnoascus destructans*, a fungal pathogen of bats, correlates with changes in microbial metacommunity structure. *Sci Rep* 2021; **11**: 11685.
4. Jiménez RR, Carfagno A, Linhoff L, Gratwicke B, Woodhams DC, Chafran LS, et al. Inhibitory bacterial diversity and mucosome function differentiate susceptibility of Appalachian salamanders to chytrid fungal infection. *Appl Environ Microbiol* 2022; **88**: e01818-21.
5. Keady MM, Jimenez RR, Bragg M, Wagner JCP, Bornbusch SL, Power ML, et al. Ecoevolutionary processes structure milk microbiomes across the mammalian tree of life. *Proc Natl Acad Sci* 2023; **120**: e2218900120.
6. Woodhams DC, Bletz MC, Becker CG, Bender HA, Buitrago-Rosas D, Diebboll H, et al. Host-associated microbiomes are predicted by immune system complexity and climate. *Genome Biol* 2020; **21**: 23.

7. Bornbusch SL, Greene LK, Rahobilalaina S, Calkins S, Rothman RS, Clarke TA, et al. Gut microbiota of ring-tailed lemurs (*Lemur catta*) vary across natural and captive populations and correlate with environmental microbiota. *Anim Microbiome* 2022; **4**: 29.

8. Rosenberg E, Zilber-Rosenberg I. Microbes drive evolution of animals and plants: The hologenome concept. *MBio* 2016; **7**: e01395-15.

9. Osborne OG, De-Kayne R, Bidartondo MI, Hutton I, Baker WJ, Turnbull CGN, et al. Arbuscular mycorrhizal fungi promote coexistence and niche divergence of sympatric palm species on a remote oceanic island. *New Phytol* 2018; **217**: 1254–1266.

10. Zhu Y-G, Xiong C, Wei Z, Chen Q-L, Ma B, Zhou S-Y-D, et al. Impacts of global change on the phyllosphere microbiome. *New Phytol* 2022; **234**: 1977–1986.

11. McKenzie VJ, Bowers RM, Fierer N, Knight R, Lauber CL. Co-habiting amphibian species harbor unique skin bacterial communities in wild populations. *ISME J* 2012; **6**: 588–596.

12. Muletz Wolz CR, Yarwood SA, Campbell Grant EH, Fleischer RC, Lips KR. Effects of host species and environment on the skin microbiome of Plethodontid salamanders. *J Anim Ecol* 2018; **87**: 341–353.

584 13. Teste FP, Kardol P, Turner BL, Wardle DA, Zemunik G, Renton M, et al. Plant-
585 soil feedback and the maintenance of diversity in Mediterranean-climate
586 shrublands. *Science* 2017; **355**: 173–176.
587 14. Muletz CR, Myers JM, Domangue RJ, Herrick JB, Harris RN. Soil
588 bioaugmentation with amphibian cutaneous bacteria protects amphibian
589 hosts from infection by *Batrachochytrium dendrobatidis*. *Biol Conserv* 2012;
590 **152**: 119–126.
591 15. Brucker RM, Bordenstein SR. The hologenomic basis of speciation: Gut
592 bacteria cause hybrid lethality in the genus *Nasonia*. *Science* 2013; **341**:
593 667–669.
594 16. Brooks AW, Kohl KD, Brucker RM, van Opstal EJ, Bordenstein SR.
595 Phylosymbiosis: Relationships and functional effects of microbial
596 communities across host evolutionary history. *PLoS Biol* 2016; **14**:
597 e2000225.
598 17. Youngblut ND, Reischer GH, Walters W, Schuster N, Walzer C, Stalder G, et
599 al. Host diet and evolutionary history explain different aspects of gut
600 microbiome diversity among vertebrate clades. *Nat Commun* 2019; **10**:
601 2200.
602 18. Song SJ, Sanders JG, Delsuc F, Metcalf J, Amato K, Taylor MW, et al.
603 Comparative analyses of vertebrate gut microbiomes reveal convergence
604 between birds and bats. *MBio* 2020; **11**: e02901-19.

19. Ross AA, Müller KM, Scott Weese J, Neufeld JD. Comprehensive skin microbiome analysis reveals the uniqueness of human skin and evidence for phylosymbiosis within the class Mammalia. *Proc Natl Acad Sci USA* 2018; **115**: E5786–E5795.

20. Doane MP, Morris MM, Papudeshi B, Allen L, Pande D, Haggerty JM, et al. The skin microbiome of elasmobranchs follows phylosymbiosis, but in teleost fishes, the microbiomes converge. *Microbiome* 2020; **8**: 93.

21. Ramírez-Barahona S, González-Serrano FM, Martínez-Ugalde E, Soto-Pozos A, Parra-Olea G, Rebollar EA. Host phylogeny and environment shape the diversity of salamander skin bacterial communities. *Anim Microbiome* 2023; **5**: 52.

22. Abdelfattah A, Tack AJM, Wasserman B, Liu J, Berg G, Norelli J, et al. Evidence for host–microbiome co-evolution in apple. *New Phytol* 2022; **234**: 2088–2100.

23. Arora J, Buček A, Hellemans S, Beránková T, Arias JR, Fisher BL, et al. Evidence of cospeciation between termites and their gut bacteria on a geological time scale. *Proc R Soc B Biol Sci* 2023; **290**: 20230619.

24. Mazel F, Davis KM, Loudon A, Kwong WK, Groussin M, Parfrey LW. Is host filtering the main driver of phylosymbiosis across the tree of life? *mSystems* 2018; **3**: e00097-18.

625 25. Ingala MR, Simmons NB, Dunbar M, Wultsch C, Krampis K, Perkins SL. You
626 are more than what you eat: Potentially adaptive enrichment of microbiome
627 functions across bat dietary niches. *Anim Microbiome* 2021; **3**: 82.
628 26. Kohl KD. Ecological and evolutionary mechanisms underlying patterns of
629 phylosymbiosis in host-associated microbial communities. *Philos Trans R*
630 *Soc B Biol Sci* 2020; **375**: 20190251.
631 27. Garcias-Bonet N, Roik A, Tierney B, García FC, Villela HDM, Dungan AM, et
632 al. Horizon scanning the application of probiotics for wildlife. *Trends*
633 *Microbiol* 2024; **32**: 252–269.
634 28. Cheng TL, Mayberry H, McGuire LP, Hoyt JR, Langwig KE, Nguyen H, et al.
635 Efficacy of a probiotic bacterium to treat bats affected by the disease white-
636 nose syndrome. *J Appl Ecol* 2017; **54**: 701–708.
637 29. Harris RN, Brucker RM, Walke JB, Becker MH, Schwantes CR, Flaherty DC,
638 et al. Skin microbes on frogs prevent morbidity and mortality caused by a
639 lethal skin fungus. *ISME J* 2009; **3**: 818–824.
640 30. Daisley BA, Pitek AP, Chmiel JA, Al KF, Chernyshova AM, Faragalla KM, et
641 al. Novel probiotic approach to counter *Paenibacillus* larvae infection in
642 honey bees. *ISME J* 2020; **14**: 476–491.
643 31. Ross AA, Rodrigues Hoffmann A, Neufeld JD. The skin microbiome of
644 vertebrates. *Microbiome* 2019; **7**: 79.

645 32. Rollins-Smith LA. The importance of antimicrobial peptides (AMPs) in
646 amphibian skin defense. *Dev Comp Immunol* 2023; **142**: 104657.
647 33. UCN/SCC Conservation Breeding Specialist Group: Apple Valley MN.
648 Proceedings of the Appalachian salamander conservation workshop. 2008.
649 34. Camp CD, Peterman WE, Milanovich JR, Lamb T, Maerz JC, Wake DB. A
650 new genus and species of lungless salamander (family Plethodontidae) from
651 the Appalachian highlands of the south-eastern United States. *J Zool* 2009;
652 **279**: 86–94.
653 35. Scheele BC, Pasmans F, Skerratt LF, Berger L, Martel A, Beukema W, et al.
654 Amphibian fungal panzootic causes catastrophic and ongoing loss of
655 biodiversity. *Science* 2019; **363**: 1459–1463.
656 36. Muletz-Wolz CR, Fleischer RC, Lips KR. Fungal disease and temperature alter
657 skin microbiome structure in an experimental salamander system. *Mol Ecol*
658 2019; **28**: 2917–2931.
659 37. Standish I, Leis E, Schmitz N, Credico J, Erickson S, Bailey J, et al.
660 Optimizing, validating, and field testing a multiplex qPCR for the detection of
661 amphibian pathogens. *Dis Aquat Organ* 2018; **129**: 1–13.
662 38. Kinney VC, Heemeyer JL, Pessier AP, Lannoo MJ. Seasonal pattern of
663 *Batrachochytrium dendrobatidis* infection and mortality in *Lithobates*
664 *areolatus*: Affirmation of Vredenburg's '10,000 zoospore rule'. *PLoS One*
665 2011; **6**: e16708.

39. Vredenburg VT, Knapp RA, Tunstall TS, Briggs CJ. Dynamics of an emerging disease drive large-scale amphibian population extinctions. *Proc Natl Acad Sci USA* 2010; **107**: 9689–9694.

40. Callahan BJ, McMurdie PJ, Rosen MJ, Han AW, Johnson AJA, Holmes SP. DADA2: High-resolution sample inference from Illumina amplicon data. *Nat Methods* 2016; **13**: 581–583.

41. Katoh K, Misawa K, Kuma K, Miyata T. MAFFT: a novel method for rapid multiple sequence alignment based on fast Fourier transform. *Nucleic Acids Res* 2002; **30**: 3059–3066.

42. Price MN, Dehal PS, Arkin AP. FastTree 2 - Approximately maximum-likelihood trees for large alignments. *PLoS One* 2010; **5**: e9490.

43. Bolyen E, Rideout JR, Dillon MR, Bokulich NA, Abnet CC, Al-Ghalith GA, et al. Reproducible, interactive, scalable and extensible microbiome data science using QIIME 2. *Nat Biotechnol* 2019; **37**: 852–857.

44. McMurdie PJ, Holmes S. Phyloseq: An R package for reproducible interactive analysis and graphics of microbiome census data. *PLoS One* 2013; **8**: e61217.

45. Davis NM, Proctor DiM, Holmes SP, Relman DA, Callahan BJ. Simple statistical identification and removal of contaminant sequences in marker-gene and metagenomics data. *Microbiome* 2018; **6**: 226.

686 46. Maidak BL, Olsen GJ, Larsen N, Overbeek R, McCaughey MJ, Woese CR.
687 The Ribosomal Database Project (RDP). *Nucleic Acids Res* 1996; **24**: 82–
688 85.
689 47. Woodhams DC, Alford RA, Antwis RE, Archer H, Becker MH, Belden LK, et al.
690 Antifungal isolates database of amphibian skin-associated bacteria and
691 function against emerging fungal pathogens. *Ecology* 2015; **96**: 595–595.
692 48. Scheirer CJ, Ray WS, Hare N. The analysis of ranked data derived from
693 completely randomized factorial designs. *Biometrics* 1976; **32**: 429–434.
694 49. Mangiafico SS. rcompanion: Functions to support extension education
695 program evaluation. R package version 2.4.30. 2023.
696 50. Ogle DH, Doll JC, Wheeler AP, Dinno A. FSA: simple fisheries stock
697 assessment methods. R package version 0.9.4. 2023.
698 51. Chen J, Zhang X, Yang L. GUniFrac: Generalized UniFrac distances,
699 distance-based multivariate methods and feature-based univariate methods
700 for microbiome data analysis. R package version 1.8. 2022.
701 52. Kembel SW, Cowan PD, Helmus MR, Cornwell WK, Morlon H, Ackerly DD, et
702 al. Picante: R tools for integrating phylogenies and ecology. *Bioinformatics*
703 2010; **26**: 1463–1464.
704 53. Muletz-Wolz CR, Barnett SE, DiRenzo GV, Zamudio KR, Toledo LF, James
705 TY, et al. Diverse genotypes of the amphibian-killing fungus produce distinct

phenotypes through plastic responses to temperature. *J Evol Biol* 2019; **32**: 287–298.

54. Liu Y, Xie J. Cauchy combination test: a powerful test with analytic p-value calculation under arbitrary dependency structures. *J Am Stat Assoc* 2020; **115**: 393–402.

55. Kumar S, Suleski M, Craig JM, Kasprowicz AE, Sanderford M, Li M, et al. TimeTree 5: An expanded resource for species divergence times. *Mol Biol Evol* 2022; **39**: msac174.

56. Paradis E, Claude J, Strimmer K. APE: Analyses of phylogenetics and evolution in R language. *Bioinformatics* 2004; **20**: 289–290.

57. Revell LJ. phytools: An R package for phylogenetic comparative biology (and other things). *Methods Ecol Evol* 2012; **3**: 217–223.

58. Legendre P, Lapointe F-J, Casgrain P. Modeling brain evolution from behavior: A permutational regression approach. *Evolution* 1994; **48**: 1487–1499.

59. Lichstein JW. Multiple regression on distance matrices: A multivariate spatial analysis tool. *Plant Ecol* 2007; **188**: 117–131.

60. Goslee SC, Urban DL. The ecodist package for dissimilarity-based analysis of ecological data. *J Stat Softw* 2007; **22**: 1–19.

61. Lim SJ, Bordenstein SR. An introduction to phylosymbiosis. *Proc R Soc B Biol Sci* 2020; **287**: 20192900.

62. Legendre P, Desdevises Y, Bazin E. A statistical test for host-parasite coevolution. *Syst Biol* 2002; **51**: 217–234.

63. Darcy JL, Amend AS, Swift SOI, Sommers PS, Lozupone CA. specificity: an R package for analysis of feature specificity to environmental and higher dimensional variables, applied to microbiome species data. *Environ Microbiomes* 2022; **17**: 34.

64. Rao CR. Diversity and dissimilarity coefficients: A unified approach. *Theor Popul Biol* 1982; **21**: 24–43.

65. Rao CR. Quadratic entropy and analysis of diversity. *Sankhya* 2010; **72**-**A**: 70–80.

66. Foster ZSL, Sharpton TJ, Grünwald NJ. Metacoder: An R package for visualization and manipulation of community taxonomic diversity data. *PLoS Comput Biol* 2017; **13**: e1005404.

67. Love MI, Huber W, Anders S. Moderated estimation of fold change and dispersion for RNA-seq data with DESeq2. *Genome Biol* 2014; **15**: 550.

68. McMurdie PJ, Holmes S. Waste not, want not: Why rarefying microbiome data is inadmissible. *PLoS Comput Biol* 2014; **10**: e1003531.

69. Requena T, Velasco M. The human microbiome in sickness and in health. *Rev Clínica Española (English Ed)* 2021; **221**: 233–240.

746 70. Olanrewaju OS, Ayangbenro AS, Glick BR, Babalola OO. Plant health:
747 feedback effect of root exudates-rhizobiome interactions. *Appl Microbiol*
748 *Biotechnol* 2019; **103**: 1155–1166.
749 71. Hammer TJ, Sanders JG, Fierer N. Not all animals need a microbiome. *FEMS*
750 *Microbiol Lett* 2019; **366**: fnz117.
751 72. van Bruggen AHC, Goss EM, Havelaar A, van Diepeningen AD, Finckh MR,
752 Morris JG. One Health - Cycling of diverse microbial communities as a
753 connecting force for soil, plant, animal, human and ecosystem health. *Sci*
754 *Total Environ* 2019; **664**: 927–937.
755 73. Trevelline BK, Fontaine SS, Hartup BK, Kohl KD. Conservation biology needs
756 a microbial renaissance: A call for the consideration of host-associated
757 microbiota in wildlife management practices. *Proc R Soc B Biol Sci* 2019;
758 **286**: 20182448.
759 74. Perez-Lamarque B, Krehenwinkel H, Gillespie RG, Morlon H. Limited evidence
760 for microbial transmission in the phylosymbiosis between hawaiian spiders
761 and their microbiota. *mSystems* 2022; **7**: e01104-21.
762 75. Bletz MC, Archer H, Harris RN, McKenzie VJ, Rabemananjara FCE,
763 Rakotoarison A, et al. Host ecology rather than host phylogeny drives
764 amphibian skin microbial community structure in the biodiversity hotspot of
765 Madagascar. *Front Microbiol* 2017; **8**: 1530.

766 76. Moen DS, Ravelojaona RN, Hutter CR, Wiens JJ. Testing for adaptive
767 radiation: A new approach applied to Madagascar frogs. *Evolution* 2021; **75**:
768 3008–3025.
769 77. Kozak KH, Wiens JJ. What explains patterns of species richness? The relative
770 importance of climatic-niche evolution, morphological evolution, and
771 ecological limits in salamanders. *Ecol Evol* 2016; **6**: 5940–5949.
772 78. Linehan JL, Harrison OJ, Han SJ, Byrd AL, Vujkovic-Cvijin I, Villarino A V., et
773 al. Non-classical immunity controls microbiota impact on skin immunity and
774 tissue repair. *Cell* 2018; **172**: 784–796.
775 79. Trujillo AL, Hoffman EA, Becker CG, Savage AE. Spatiotemporal adaptive
776 evolution of an MHC immune gene in a frog-fungus disease system.
777 *Heredity* 2021; **126**: 640–655.
778 80. Rovito SM, Parra-Olea G, Vásquez-Almazán CR, Papenfuss TJ, Wake DB.
779 Dramatic declines in neotropical salamander populations are an important
780 part of the global amphibian crisis. *Proc Natl Acad Sci U S A* 2009; **106**:
781 3231–3236.
782 81. Cheng TL, Rovito SM, Wake DB, Vredenburg VT. Coincident mass extirpation
783 of neotropical amphibians with the emergence of the infectious fungal
784 pathogen *Batrachochytrium dendrobatidis*. *Proc Natl Acad Sci U S A* 2011;
785 **108**: 9502–9507.

786 82. Dawood MAO, Koshio S, Abdel-Daim MM, Van Doan H. Probiotic application
787 for sustainable aquaculture. *Rev Aquac* 2019; **11**: 907–924.
788 83. Jiménez-Gómez A, Celador-Lera L, Fradejas-Bayón M, Rivas R. Plant
789 probiotic bacteria enhance the quality of fruit and horticultural crops. *AIMS*
790 *Microbiol* 2017; **3**: 483–501.
791 84. Bjarnason I, Sission G, Hayee BH. A randomised, double-blind, placebo-
792 controlled trial of a multi-strain probiotic in patients with asymptomatic
793 ulcerative colitis and Crohn's disease. *Inflammopharmacology* 2019; **27**:
794 465–473.
795 85. Kueneman JG, Woodhams DC, Harris R, Archer HM, Knight R, McKenzie VJ.
796 Probiotic treatment restores protection against lethal fungal infection lost
797 during amphibian captivity. *Proc R Soc B Biol Sci* 2016; **283**: 20161553.
798 86. Muletz-Wolz CR, DiRenzo GV, Yarwood SA, Grant EHC, Fleischer RC, Lips
799 KR. Antifungal bacteria on woodland salamander skin exhibit high taxonomic
800 diversity and geographic variability. *Appl Environ Microbiol* 2017; **83**:
801 e00186-17.
802 87. Becker MH, Brophy JAN, Barrett K, Bronikowski E, Evans M, Glassey E, et al.
803 Genetically modifying skin microbe to produce violacein and augmenting
804 microbiome did not defend Panamanian golden frogs from disease. *ISME*
805 *Commun* 2021; **1**: 57.

806 88. Mu J, Li X, Jiao J, Ji G, Wu J, Hu F, et al. Biocontrol potential of vermicompost
807 through antifungal volatiles produced by indigenous bacteria. *Biol Control*
808 2017; **112**: 49–54.
809 89. Knapp RA, Joseph MB, Smith TC, Hegeman EE, Vredenburg VT, Erdman JE,
810 et al. Effectiveness of antifungal treatments during chytridiomycosis
811 epizootics in populations of an endangered frog. *PeerJ* 2022; **10**: e12712.
812 90. Küng D, Bigler L, Davis LR, Gratwicke B, Griffith E, Woodhams DC. Stability of
813 microbiota facilitated by host immune regulation: Informing probiotic
814 strategies to manage amphibian disease. *PLoS One* 2014; **9**: e87101.
815 91. Muletz-Wolz CR, Almario JG, Barnett SE, DiRenzo GV, Martel A, Pasmans F,
816 et al. Inhibition of fungal pathogens across genotypes and temperatures by
817 amphibian skin bacteria. *Front Microbiol* 2017; **8**: 1551.
818 92. Torres-Sánchez M, Longo A V. Linking pathogen–microbiome–host
819 interactions to explain amphibian population dynamics. *Mol Ecol* 2022; **31**:
820 5784–5794.
821 93. Alexiev A, Chen MY, Korpita T, Weier AM, McKenzie VJ. together or alone:
822 evaluating the pathogen inhibition potential of bacterial cocktails against an
823 amphibian pathogen. *Microbiol Spectr* 2023; **11**: e01518-22.
824

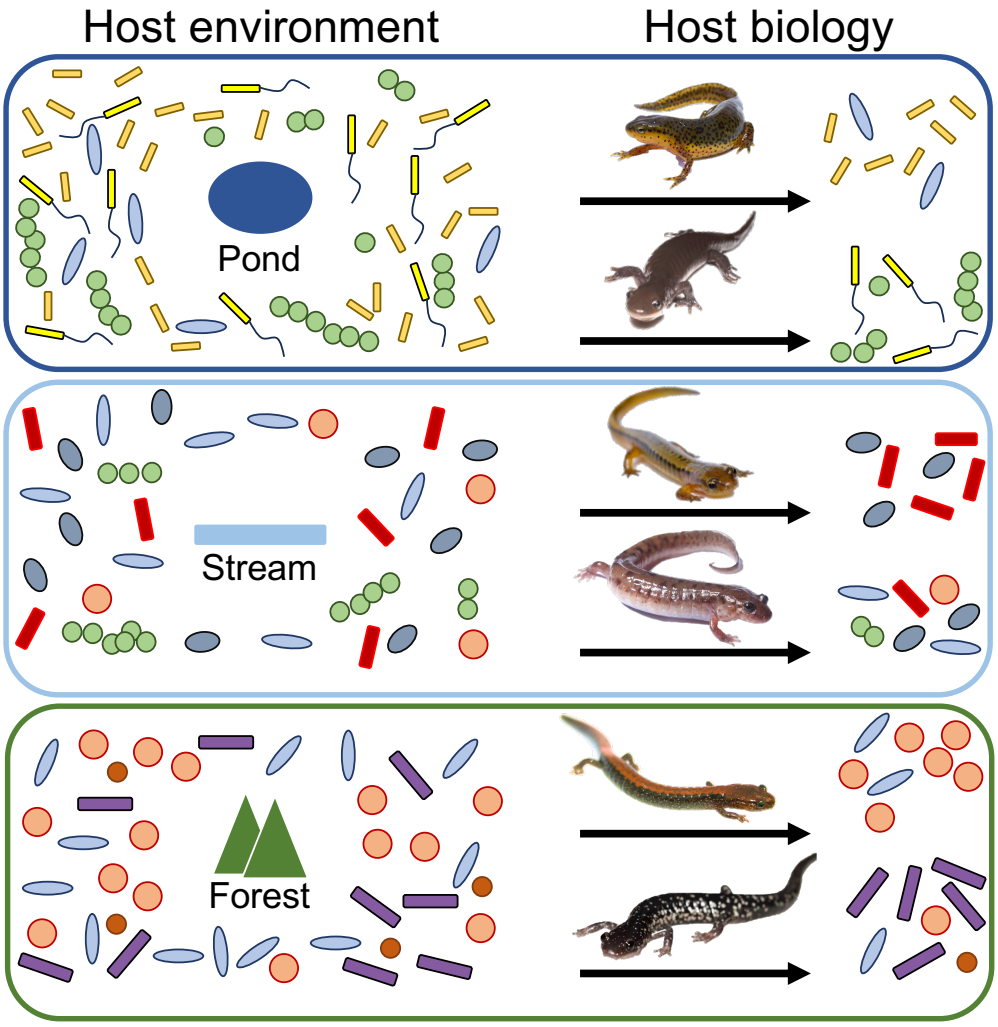

Figure 1. Conceptual diagram illustrating how host environment impacts the regional pool of microbes, whereas species-specific host traits filter this pool of microbes.

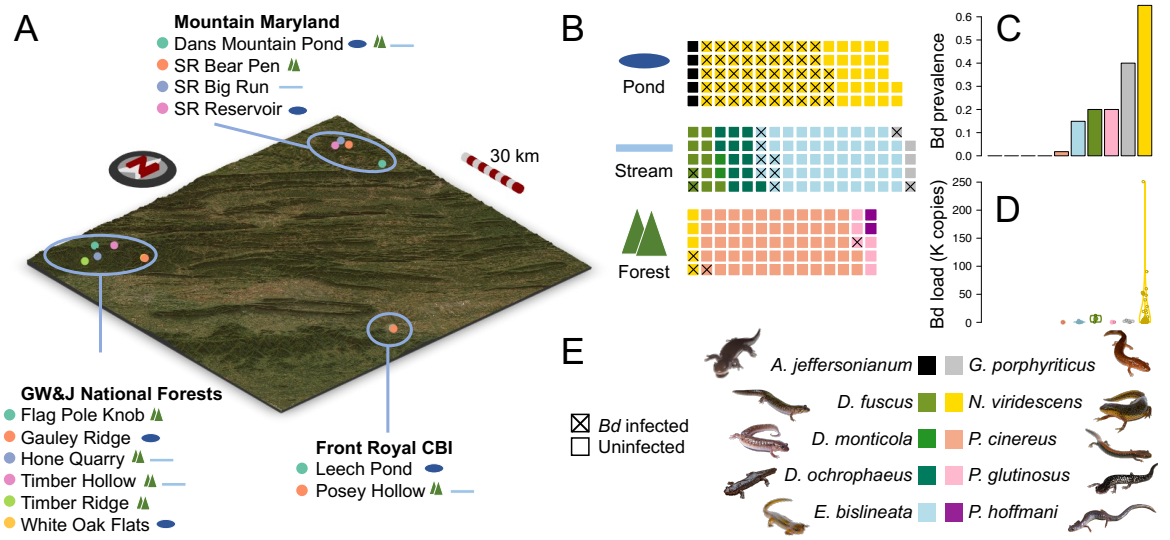

Figure 2: Sampling scheme. Sampling sites within each of the three localities: Mountain Maryland, George Washington and Jefferson National Forests and Front Royal Conservation Biology Institute, are shown on a topological map (A). Sites are distinguished by point colour within each locality, and habitat types are shown as icons (as in panel B) to the right of each site name. Waffle plots (B) show the number of individuals of each species in each habitat type. Each square represents one individual, coloured by species as in panel E. *Batrachochytrium dendrobatidis* (Bd) infected individuals are indicated by a cross. Bd prevalence is shown as a bar plot (panel C; proportion of infected individuals) and Bd load is shown as a violin plot (panel D; units of 1,000 copies; jittered points show actual values for all infected individuals). Bars and violins are coloured by species as in E. Photographs in E are all the authors' work except for *P. hoffmani*, which is available on a creative commons licence (CC-BY-NC, © Josh Emms 2018).

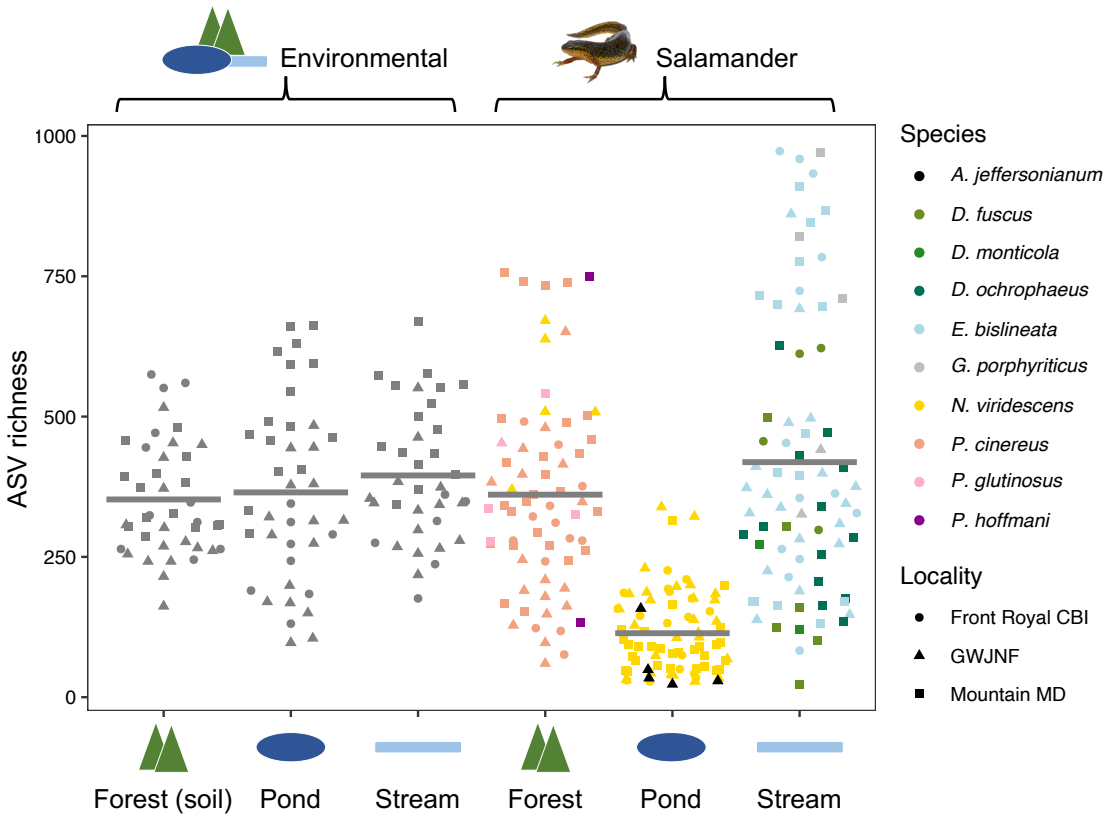

844

845 Figure 3: Alpha diversity for all samples. Beeswarm plots show ASV richness for all
846 environmental (left) and salamander skin samples (right), grouped by habitat on the x-
847 axis. Each point represents a single sample and points with similar ASV richness
848 values are separated on the X-axis to minimise overlap. Horizontal bars show the
849 mean for each habitat. Point colour indicates host species and shape indicates locality.

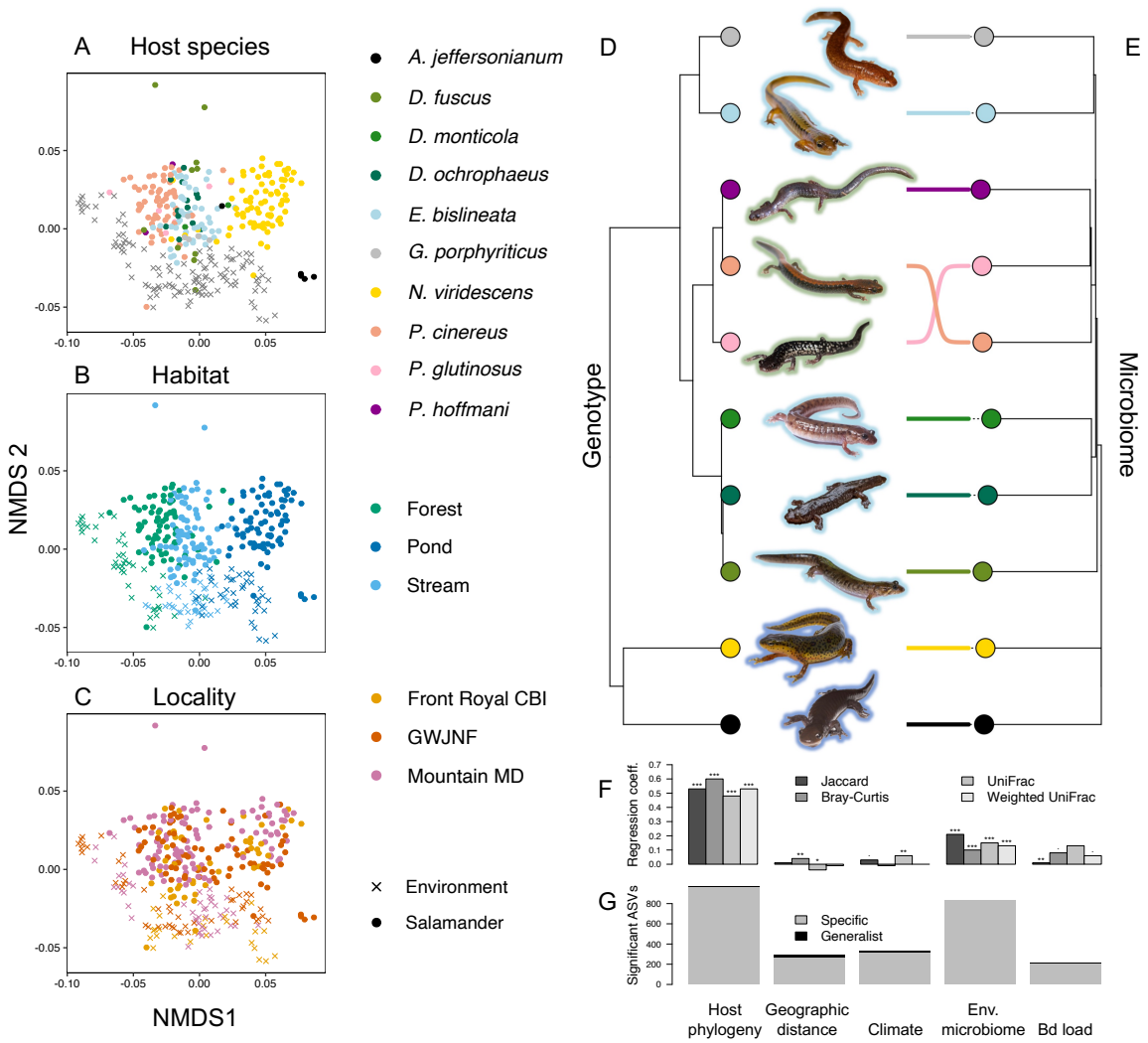

Figure 4: There is a strong signal of phylosymbiosis in Appalachian salamander skin microbiomes. NMDS plots based on Bray-Curtis distance (A-C) for all salamander skin and environmental samples. Each point represents a single sample and points are coloured by host species (A), habitat (B), or locality (C). Point shapes show sample type (i.e. salamander skin or environmental samples). A dated host phylogeny (D) is shown beside neighbour-joining based hierarchical clustering of mean pairwise Bray-Curtis microbiome distance between each salamander species pair (E). Coloured lines link the same species between the two dendrograms. Coloured tip points indicate

859 species, and outlines around salamander images indicate primary habitat (green:
860 forest, dark blue: pond, light blue: stream). Results of multiple regression on distance
861 matrices (MRM) analysis (F) show the effect of multiple explanatory variables of skin
862 microbiome distance. Bar plots show standardised regression coefficients for host
863 phylogeny, geographic distance, climate distance, environmental microbiome
864 distance, and Bd load using four different skin-microbiome beta-diversity statistics.
865 Stars above each bars indicate significance ($P < 0.001$: ***; $P < 0.01$: **; $P < 0.05$: *).
866 In our specificity analysis (G), there were most significantly specific ASVs for host
867 phylogeny, followed by environmental microbiome distance.
868

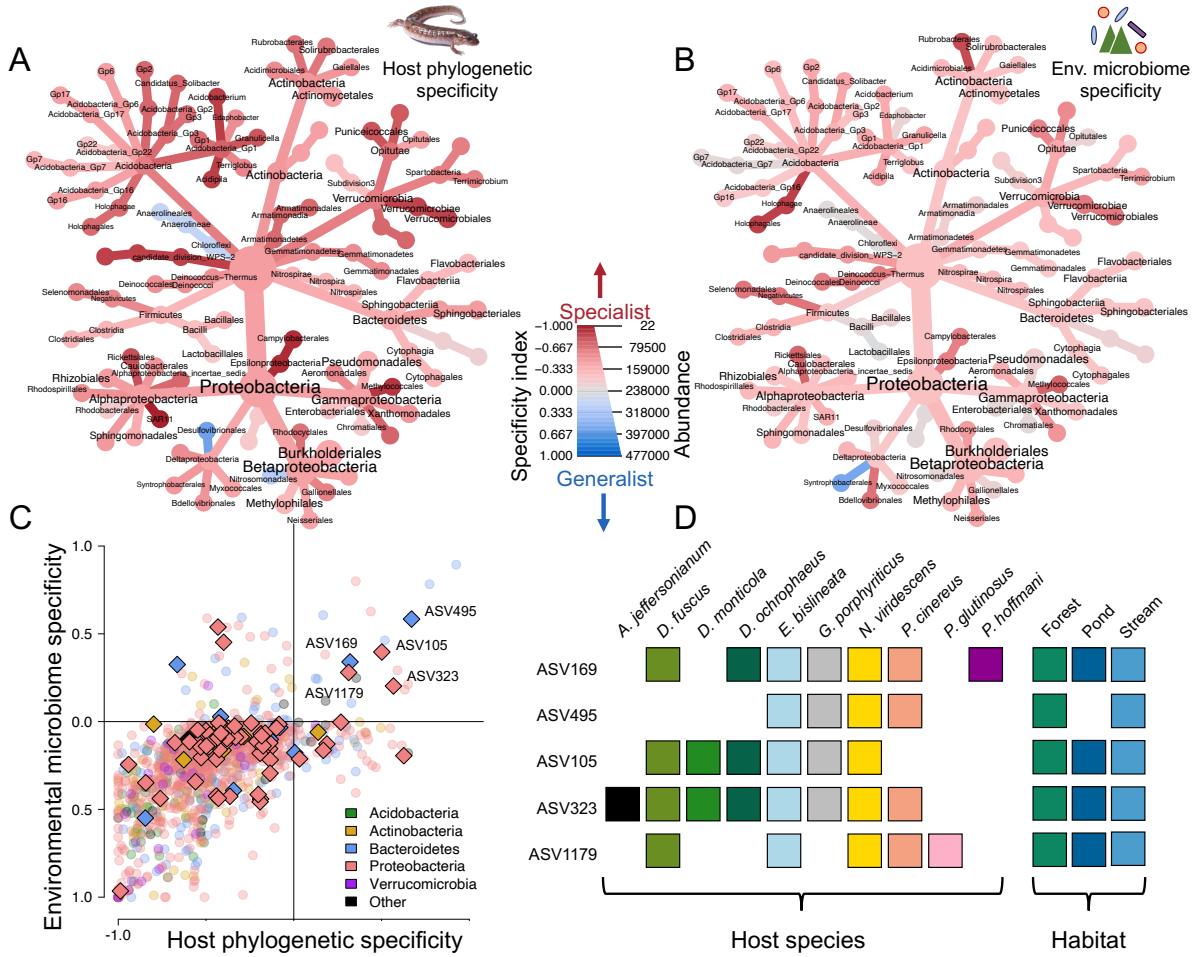

Figure 5: Host and environmental specificity across the salamander skin microbiome and in known anti-Bd taxa. The bacterial phylogeny of the skin microbiome is shown to order level, with colour indicating mean specificity index to host phylogeny (A) and environmental microbiome distance (B). A specificity index < 0 indicates higher specificity and specificity index > 0 indicates higher generalism. The dot plot (C) shows the relationship between these metrics with each point representing a single ASV, coloured by phylum. Known anti-Bd ASVs are shown as diamonds and all other ASVs are shown as circles. Known anti-Bd taxa with the lowest specificity (i.e. most positive specificity index) are present in a wide range of host species and habitats (D).

880 Coloured squares indicate presence in each host species and habitat for the most
881 generalist anti-Bd ASVs.